# Decentralized Direct Localization Based on Gauss-Newton Method in Multi-Sensor Networks

Guoxin Zhang*, Yunfei Liang*, Cong Wang*, Wei Yi*, Hien Quoc Ngo†,
Michail Matthaiou†, and Pramod K. Varshney*
*School of Information and Communication Engineering, University of Electronic Science and Technology of China, P. R. China
†Centre for Wireless Innovation (CWI), Queen's University Belfast, U.K.
*Department of Electrical Engineering and Computer Science, Syracuse University, USA
Email: brucezgx@163.com

***Abstract*—Traditional centralized direct localization methods require the transmission of the complete baseband signal to the fusion center (FC) for target localization. Due to the limited communication bandwidth as well as energy required in transmission, this centralized framework is not suitable for large-scale sensor networks. This paper proposes an information-driven decentralized direct localization framework. Firstly, a maximum-likelihood position estimator, based on the Gauss-Newton method, is derived. Then, a decentralized implementation framework is constructed. At its core, there is no dedicated FC while the sensors transmit information to their neighboring nodes only through single hops, achieving target localization through iterative processes based on the concept of consensus. Simulation results confirm the stability and robustness of the proposed method in different scenarios.**

***Index Terms*—Consensus, decentralized estimation, direct localization, Gauss-Newton method, maximum-likelihood estimation.**

## I. Introduction

Multi-sensor networks have attracted increasing attention and have demonstrated considerable potential [1], particularly in the realms of target detection [2], tracking [3], and localization [4]. The integration of information across multiple sensors empowers these networks to surpass the performance capabilities achievable by individual nodes in isolation. This collaborative synergy not only enriches the quality of gathered data but also plays a pivotal role in enhancing the overall effectiveness and robustness of the system across a spectrum of applications.

Target localization, as a core representative task in the space of multi-sensor applications, is currently attracting noticeable research attention. Generally, target localization techniques can be categorized into two main types [4], [5], [8]–[10]: two-step localization methods [4]–[7] and direct localization methods [8]–[10]. The first type of localization process typically involves two steps: initially, measurements pertinent to position estimation (such as angle of arrival or time of delay) are collected to detect potential targets at each sensor node. Subsequently, the target position is computed by solving a set of equations based on these measurements. These methods are often termed as two-step localization approaches, which involves first the detection of a target based on measurements and then its localization. However, following the detection phase, certain sensors may not receive position-related measurements due to varying path attenuation and signal strength fluctuations. This results in challenges in associating targets with measurements that could eventually undermine the localization performance. On the other hand, another category of localization algorithms, known as direct localization approaches, aims to directly localize the target by jointly processing the unthresholded signal echoes and obtaining maximum-likelihood estimates (MLE). The direct localization approach leverages the complete received signal information and eliminates the need for the target-measurement association step present in the two-step localization approach. Therefore, it tends to offer more robust localization performance, particularly in scenarios with low signal-to-noise ratios (SNRs) [10].

However, the direct localization approach faces significant challenges, particularly in terms of communication load on the FC, as it requires the transmission of complete baseband signals [8]. This challenge becomes more pronounced with a surge in the number of sensors, such as in large-scale sensor networks [11]. Moreover, in the context of target localization addressed in this paper, where the measurements from all the sensors need to be processed by the FC for target position estimation, a centralized system faces the risk of breakdown if the FC is compromised as it provides a single point of failure. This vulnerability poses a significant hindrance to meeting the demands of flexible deployment and rapid response inherent in multi-sensor networks. To address the potential drawbacks mentioned above, a decentralized framework has emerged [12], [13]. At its core, the completion of system tasks in a decentralized system does not require the involvement of a FC, instead, it relies on information exchange among nodes and their neighbors.

Due to the robustness of the system structure and the high resilience of signal processing frameworks, decentralized systems have been the subject of extensive research in recent years [13], [15]–[17]. Soatti *et al*. [18] addressed the problem of decentralized localization using signal strength information and developed a target localization algorithm under a

decentralized least squares framework. Similarly, within this framework, Wu *et al*. [19] noticed the potential SNR variations across different sensors, leading to measurements of varying qualities. They utilized game theory principles to assign different weights to measurements from different sensors, achieving higher localization performance gains compared to fixed-weight methods. While the aforementioned algorithms employ a two-step localization method, their performance is not entirely satisfactory in low SNR scenarios. Xia *et al*. [20] developed an adaptive iterative decentralized direct localization algorithm under the steepest descent framework, which outperforms two-step localization algorithms in terms of localization performance. However, this algorithm relies on the choice of parameters, such as step size. Pourhomayoun *et al*. [21] proposed three different decentralized direct localization methods. The first method applies the Gershgorin theorem to compute the intermediate localization results, which are then fused into a common sensor to achieve target position estimation. This method requires the transmission of original signal samples, resulting in a significant communication load. The second method involves computing the cross ambiguity matrices (CAM) and conducting multi-hop transmissions in a sensor network. This method still demands substantial communication bandwidth and requires frequent communication between sensors. The third method uses some extracted time-difference-of-arrival or frequency-difference-of-arrival values to aid in the formation of the CAM and then extracts the position from the CAM via the largest eigenvalues. In comparison to the former two methods, the third method yields less satisfactory localization accuracy. Ma *et al*. [22] constructed a local direct localization cost function at each sensor node and utilized importance sampling methods to complete the target position estimation. However, this method requires accurate interpolation fitting of the objective function, resulting in high computational complexity.

This paper proposes a novel decentralized direct localization (DDL) architecture, whose main objective is to not only enhance the system robustness but also reduce the communication load compared to traditional centralized direct localization methods (e.g., [9], [10]). The main contributions of our work are as follows:

1) A new single-node iterative estimation method for direct localization is developed. Drawing inspiration from the Gauss-Newton method, the centralized direct localization estimator is decomposed, allowing each local sensor to independently perform direct position estimation similar to the centralized approach. This methodology eliminates the need for a FC's involvement in the entire system. In addition, direct localization, based on the particle swarm optimization (PSO) algorithm, is introduced into the position initialization process, ensuring satisfactory system efficiency while enhancing its robustness under low SNR conditions.
2) A decentralized direct localization strategy based on consensus is proposed, which moves away from traditional centralized methods that require each sensor to transmit complete baseband signals. Through an average consensus strategy, each sensor only needs to transmit low-dimensional information parameters among neighboring nodes, which significantly reduces the overall communication load of the system while effectively leveraging the relevant information from the entire system.

*Notations:* Throughout this paper, $a$ (or $A$), $\mathbf{a}$, and $\mathbf{A}$ represent scalars, vectors and matrices, respectively; $[\cdot]^\top$ denotes the transpose of its argument; $\|\cdot\|_2$ represents the 2-norm of a vector; $(\cdot)^*$ denotes the conjugate, and $(\cdot)^H$ denotes the conjugate transpose. The superscript $(\cdot)^{R(I)}$ represents the real or imaginary parts of a complex element; $\nabla_a$ is the gradient with respect to $a$. The symbol $\propto$ denotes directly proportional, while $\mathbb{E}\{\cdot\}$ denotes the mathematical expectation.

## II. System Configuration and Signal Model

In this paper, we study the problem of position estimation in a two-dimensional Cartesian coordinate system using a decentralized multi-sensor system. We assume that the system is equipped with $L$ sensor nodes that passively receive signals from a radiation source to perceive the target, while the system clock synchronization among them is guaranteed using devices, such as a GPS unit. Compared to a centralized architecture, a decentralized system does not require the involvement of a FC. In this architecture, each sensor node can only communicate with its neighboring nodes, as shown in Fig. 1. Denote the position of the unknow radiation source by the vector of coordinates, $\boldsymbol{u} = (x,y)^\top$. The position of the $l$-th sensor node is denoted by the vector of coordinates, $\boldsymbol{p}_l = (x_l, y_l)^\top, l = 1,\ldots,L$. We also assume that the signal propagates along the line of sight (LoS). The baseband signal observed by the $l$-th sensor can be represented as

$$r_l(t) = \alpha_l s(t - \tau_l(\boldsymbol{u})) + n_l(t),\ 0 < t < T, \tag{1}$$

where $T$ is the observation interval. The term $\alpha_l$ is an unknown complex scalar representing the path loss. The term $s(t)$ is the transmitted signal waveform from the target. The term $\tau_l(\boldsymbol{u})$ represents the propagation delay from the source signal to the $l$th sensor, which can be defined as

$$\tau_l(\boldsymbol{u}) = \frac{\|\boldsymbol{p}_l - \boldsymbol{u}\|_2}{c} = \frac{\sqrt{(x-x_l)^2 + (y-y_l)^2}}{c}, \tag{2}$$

with $c$ is the speed of light. The term $n_l(t)$ represents the noise, modeled as a complex Gaussian white random process with zero mean and variance $\sigma_w^2$, and is assumed to be independent of noise at the other sensors. It is worth noting that for sensors with functionalities, such as angle or velocity measurements, the received signal model in (1) may have a more complex form. However, since the focus of this paper is not on the signal form, we only consider a simpler form involving merely time delay.

After sampling, the continuous signal of (1) can be written in a vector form

$$\mathbf{r}_l = \alpha_l \mathbf{s}(\boldsymbol{u}) + \mathbf{n}_l, \tag{3}$$

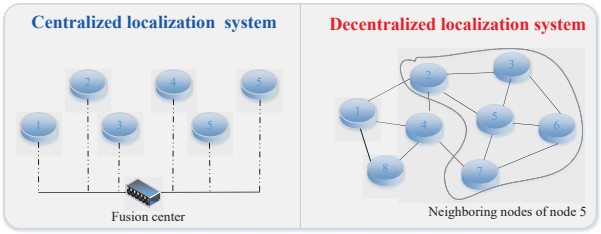


Fig. 1. Conceptual diagram of centralized and decentralized systems.

where

$$\begin{aligned}\mathbf{s}(\boldsymbol{u}) &\triangleq [s[0], s[1], \ldots, s[K-1]]^{\top},\\ \mathbf{r}_l &\triangleq [r_l[0], r_l[1], \ldots, r_l[K-1]]^{\top},\\ \mathbf{n}_l &\triangleq [n_l[0], n_l[1], \ldots, n_l[K-1]]^{\top},\end{aligned} \tag{4}$$

with the sampling interval $T_s = T/(K-1)$. The sampled noise term $\mathbf{n}_l$ is still regarded as a zero-mean complex Gaussian random vector with the correlation matrix

$$\mathbf{N}_l = \mathbb{E}\left\{\mathbf{n}_l \mathbf{n}_l^H\right\} = \sigma_l^2 \mathbf{I}_K, \tag{5}$$

where $\mathbf{I}_d$ denotes the $d \times d$ identity matrix.

## III. Centralized Direct Localization

In this section, we review the traditional direct localization algorithm with a FC based on the MLE. Note that the position information of the target is contained in the time delay of the signal. Based on the independence of the noise distribution among various sensors, the likelihood function of multi-sensor joint estimation can be expressed as

$$\zeta(\mathbf{R}|\boldsymbol{u}, \boldsymbol{\alpha}) = \gamma \prod_{l=1}^{L} \exp\left\{-\frac{1}{2}\left(\mathbf{r}_l - \alpha_l \mathbf{s}(\boldsymbol{u})\right)^H \mathbf{N}_l^{-1}\left(\mathbf{r}_l - \alpha_l \mathbf{s}(\boldsymbol{u})\right)\right\}, \tag{6}$$

where $\mathbf{R} \triangleq [\mathbf{r}_1, \ldots, \mathbf{r}_L]^{\top} \in \mathbb{C}^{L\times K}$, and $\boldsymbol{\alpha} \triangleq [\alpha_1, \ldots, \alpha_L]^{\top}$. The term $\gamma$ denotes a constant coefficient unrelated to the parameter of interest $\boldsymbol{u}$. In the following, $\boldsymbol{u}$ is omitted in $\mathbf{s}(\boldsymbol{u})$ for ease of notation, i.e., $\mathbf{s}(\boldsymbol{u})$ is written as $\mathbf{s}$. Note that the likelihood function in (6) contains two types of unknown parameters, namely the target position $\boldsymbol{u}$ and the propagation coefficient $\boldsymbol{\alpha}$. In classical centralized direct localization methods, the unknown parameter $\boldsymbol{\alpha}$ can be eliminated in (6) by using its MLE [9]. The target position can thus be estimated as

$$\hat{\boldsymbol{u}} = \arg\max_{\boldsymbol{u}} \ln \zeta(\mathbf{R}|\boldsymbol{u}). \tag{7}$$

The above equation can be solved to obtain the target position estimate through a simple grid search [9]. Note that, in the classical direct localization architectures [8]–[10], in order to acquire target localization, each sensor node needs to transmit its received baseband signal to the FC. With an increase in the number of sensor nodes, especially in large-scale networks, the communication and computational burden on the FC would become substantial. Furthermore, the aforementioned estimation process must be completed at a FC. As indicated earlier, central computation at the FC may result in a single point of system failure in the case of FC malfunction or adversarial attack. Next, we will explore the decentralized implementation of direct target localization.

## IV. Decentralized Direct Localization Framework

In this section, we propose a novel decentralized direct localization method. First, we derive an iterative estimation method for each local sensor to solve the target position based on the Gauss-Newton approach. Subsequently, we develop a decentralized multi-sensor direct localization method based on a consensus strategy.

### A. Local Iterative Estimation Process

In order to achieve the decentralized estimation of target positions, we first derive the decentralized estimation process for each local sensor node. For a given target position $\boldsymbol{u}$, the observation models of sensor $l$ under hypothesis $H_0$ (the target is absent) and $H_1$ (the target is present) are formulated as

$$H_1 : \mathbf{r}_l = \alpha_l \mathbf{s} + \mathbf{n}_l, \quad H_0 : \mathbf{r}_l = \mathbf{n}_l, \tag{8}$$

while the likelihood function of node observations under both hypotheses is given by

$$\begin{aligned}\ell(\mathbf{r}_l|\boldsymbol{u}, \alpha_l, H_1) &= \mu_1 \exp\left\{-\frac{1}{2}\left(\mathbf{r}_l - \alpha_l \mathbf{s}\right)^H \mathbf{N}_l^{-1}\left(\mathbf{r}_l - \alpha_l \mathbf{s}\right)\right\}.\\ \ell(\mathbf{r}_l|H_0) &= \mu_0 \exp\left\{-\frac{1}{2}\mathbf{r}_l^H \mathbf{N}_l^{-1} \mathbf{r}_l\right\}.\end{aligned} \tag{9}$$

where $\mu_1$, $\mu_0$ denote constant coefficients unrelated to the parameters $\boldsymbol{u}$ under hypotheses $H_1$, $H_0$ respectively. Since $\ell(\mathbf{r}_l|H_0)$ is not a function of $\boldsymbol{u}$, for the estimation of $\boldsymbol{u}$, the likelihood function can be expressed as

$$\begin{aligned}\ell(\mathbf{r}_l|\boldsymbol{u}, \alpha_l) &\propto \ln \frac{\ell(\mathbf{r}_l|\boldsymbol{u}, \alpha_l, H_1)}{\ell(\mathbf{r}_l|H_0)}\\ &= \frac{1}{2}\left\{\mathbf{r}_l^H \mathbf{N}_l^{-1} \mathbf{s}\alpha_l + \left(\alpha_l \mathbf{s}\right)^H \mathbf{N}_l^{-1} \mathbf{r}_l - \left(\alpha_l \mathbf{s}\right)^H \mathbf{N}_l^{-1} \mathbf{s}\alpha_l\right\}.\end{aligned} \tag{10}$$

For any parameter $\boldsymbol{u}$, the likelihood function (10) is maximized using $\alpha_l = \hat{\alpha}_l$, where $\hat{\alpha}_l$ is calculated as the solution to

$$\nabla_{\alpha_l} \ell(\mathbf{r}_l|\boldsymbol{u}, \alpha_l)|_{\alpha_l = \hat{\alpha}_l} = 0. \tag{11}$$

By taking the partial derivatives of the real part $\alpha_l^R$ and the imaginary part $\alpha_l^I$, (11) can be solved as

$$\nabla_{\alpha_l^R} \ell(\mathbf{r}_l|\boldsymbol{u}, \alpha_l) = \nabla_{\alpha_l^I} \ell(\mathbf{r}_l|\boldsymbol{u}, \alpha_l) = 0. \tag{12}$$

By using (10), $\nabla_{\alpha_l^R} \ell(\mathbf{r}_l|\boldsymbol{u}, \alpha_l) = 0$ becomes

$$\frac{1}{2}\left\{\mathbf{r}_l^H \mathbf{N}_l^{-1} \mathbf{s} + \mathbf{s}^H \mathbf{N}_l^{-1} \mathbf{r}_l - 2\alpha_l^R \mathbf{s}^H \mathbf{N}_l^{-1} \mathbf{s}\right\} = 0. \tag{13}$$

Similarly, by using (10), $\nabla_{\alpha_l^I} \ell(\mathbf{r}_l|\boldsymbol{u}, \alpha_l) = 0$ becomes

$$\frac{j}{2}\left\{\mathbf{r}_l^H \mathbf{N}_l^{-1} \mathbf{s} - \mathbf{s}^H \mathbf{N}_l^{-1} \mathbf{r}_l + 2j\alpha_l^I \mathbf{s}^H \mathbf{N}_l^{-1} \mathbf{s}\right\} = 0. \tag{14}$$

Combining (13) with (14) and after some simplifications, the MLE of $\alpha_l$ can be calculated as

$$\hat{\alpha}_l = \frac{\mathbf{s}^H \mathbf{N}_l^{-1} \mathbf{r}_l}{\mathbf{s}^H \mathbf{N}_l^{-1} \mathbf{s}}. \tag{15}$$

In order to obtain the likelihood of the $l$th sensor node without $\alpha_l$, we insert (15) into (10), and we obtain

$$\ell(\mathbf{r}_l|\boldsymbol{u}) = \frac{1}{2} \mathbf{r}_l^H \mathbf{N}_l^{-1} \mathbf{s} \left(\mathbf{s}^H \mathbf{N}_l^{-1} \mathbf{s}\right)^{-1} \mathbf{s}^H \mathbf{N}_l^{-1} \mathbf{r}_l. \tag{16}$$

At this point, we have obtained the local likelihood function characterization for each sensor. The target position can be determined by solving the following optimization problem:

$$\begin{aligned} &\hat{\boldsymbol{u}}_l = \arg\max_{\boldsymbol{u}} \ell(\mathbf{r}_l|\boldsymbol{u}), \\ &\text{s.t. } \ell(\mathbf{r}_l|\hat{\boldsymbol{u}}_l) \geq \kappa, \end{aligned} \tag{17}$$

where $\kappa$ is a detection threshold determined under the Bayesian or Neyman-Pearson formulation. If the log-likelihood function exceeds $\kappa$, detection of the target is declared, otherwise no target is declared.

To obtain the local target position estimates, unlike the computationally expensive grid search employed in traditional direct localization [9], [10], we, instead, utilize the principles of the Gauss-Newton algorithm. This enables a more efficient iterative estimation process for the target position at each local sensor. Denote

$$\Lambda_l \triangleq \mathbf{r}_l^H \mathbf{N}_l^{-1} \mathbf{s}, \ \Xi_l \triangleq \mathbf{s}^H \mathbf{N}_l^{-1} \mathbf{s}. \tag{18}$$

From (16) and (18), it can be observed that the local likelihood function is only related to $\Lambda_l$ and $\Xi_l$. Therefore, unlike directly expanding $\ell(\mathbf{r}_l|\boldsymbol{u})$ in (16) using a Taylor series, we perform a first-order Taylor expansion only for $\Lambda_l$ and $\Xi_l$ at the current estimate value $\hat{\boldsymbol{u}}_l^q = \left[\hat{x}_l^q, \hat{y}_l^q\right]^\top$ to obtain their approximations, where $q$ represents the number of iterations. The potential benefit of doing this is that we can effectively eliminate the need for computationally expensive operations, like calculating second-order derivatives required by the traditional Newton's method. Additionally, we can avail of faster convergence performance compared to the traditional steepest descent method. Thus, (16) can be approximated as

$$\begin{aligned} \ell(\mathbf{r}_l|\boldsymbol{u}) \propto & \frac{1}{2} \left[ \left( \nabla_{\hat{\boldsymbol{u}}_l^q} \Lambda_l \left(\hat{\boldsymbol{u}}_l^q\right) \right)^\top \triangle_{\hat{\boldsymbol{u}}_l^q} + \Lambda_l \left(\hat{\boldsymbol{u}}_l^q\right) \right] \\ & \times \left[ \left( \nabla_{\hat{\boldsymbol{u}}_l^q} \Xi_l \left(\hat{\boldsymbol{u}}_l^q\right) \right)^\top \triangle_{\hat{\boldsymbol{u}}_l^q} + \Xi_l \left(\hat{\boldsymbol{u}}_l^q\right) \right]^{-1} \\ & \times \left[ \left( \nabla_{\hat{\boldsymbol{u}}_l^q} \Lambda_l \left(\hat{\boldsymbol{u}}_l^q\right) \right)^\top \triangle_{\hat{\boldsymbol{u}}_l^q} + \Lambda_l \left(\hat{\boldsymbol{u}}_l^q\right) \right]^H. \end{aligned} \tag{19}$$

For the sake of notational convenience, $\Lambda_l^q$ is substituted for $\Lambda_l\left(\hat{\boldsymbol{u}}_l^q\right)$, while $\Xi_l^q$ is substituted for $\Xi_l\left(\hat{\boldsymbol{u}}_l^q\right)$ in the following. The components in (19) can be solved as

$$\triangle_{\hat{\boldsymbol{u}}_l^q} = \boldsymbol{u} - \hat{\boldsymbol{u}}_l^q, \tag{20}$$

$$\nabla_{\hat{\boldsymbol{u}}_l^q} \Lambda_l^q = \left[ \nabla_{\hat{x}_l^q} \Lambda_l^q, \nabla_{\hat{y}_l^q} \Lambda_l^q \right]^\top. \tag{21}$$

$$\nabla_{\hat{\boldsymbol{u}}_l^q} \Xi_l^q = \left[ \nabla_{\hat{x}_l^q} \Xi_l^q, \nabla_{\hat{y}_l^q} \Xi_l^q \right]^\top. \tag{22}$$

According to (2), the derivative of position in (21) can be transformed into a more intuitive derivative with respect to time delay as

$$\nabla_{\hat{x}_l^q} \Lambda_l^q = \nabla_{\tau_l^q} \Lambda_l^q a_l^q, \ \nabla_{\hat{y}_l^q} \Lambda_l^q = \nabla_{\tau_l^q} \Lambda_l^q b_l^q, \tag{23}$$

$$\nabla_{\hat{x}_l^q} \Xi_l^q = \nabla_{\tau_l^q} \Xi_l^q a_l^q, \ \nabla_{\hat{y}_l^q} \Xi_l^q = \nabla_{\tau_l^q} \Xi_l^q b_l^q, \tag{24}$$

where

$$\begin{aligned} a_l^q &= \nabla_{\hat{x}_l^q} \tau_l^q = \frac{\hat{x}_l^q - x_l}{c \left\| \hat{\boldsymbol{u}}_l^q - \boldsymbol{p}_l \right\|_2}, \\ b_l^q &= \bigtriangledown_{\hat{y}_l^q} \tau_l^q = \frac{\hat{y}_l^q - y_l}{c \left\| \hat{\boldsymbol{u}}_l^q - \boldsymbol{p}_l \right\|_2}. \end{aligned} \tag{25}$$

From (20), we see that the estimation of the target position $\boldsymbol{u}$ can be realized through an iterative process of $\hat{\boldsymbol{u}}_l^q$, where the increment of the iteration is determined by $\triangle_{\hat{\boldsymbol{u}}_l^q}$. Thus, after obtaining the initial value of $\hat{\boldsymbol{u}}_l^q$ for the current iteration, the key lies in how to select an appropriate increment $\triangle_{\hat{\boldsymbol{u}}_l^q}$.

The MLE of the increment between the iterative value and the true value of the target position in (19) can be obtained by solving

$$\begin{aligned} \hat{\triangle}_{\hat{\boldsymbol{u}}_l^q} &= \arg_{\triangle_{\hat{\boldsymbol{u}}_l^q}} \left\{ \frac{\partial \ \ell(\mathbf{r}_l|\boldsymbol{u})}{\partial \triangle_{\hat{\boldsymbol{u}}_l^q}} = 0 \right\} \\ &= - \left[ \mathrm{Re} \left\{ \left( \nabla_{\hat{\boldsymbol{u}}_l^q} \Lambda_l^q \right)^* \left( \nabla_{\hat{\boldsymbol{u}}_l^q} \Lambda_l^q \right)^\top \right\} \right]^{-1} \\ &\quad \times \left[ \nabla_{\hat{\boldsymbol{u}}_l^q} \Xi_l^q \ell(\hat{\boldsymbol{u}}_l^q) - \mathrm{Re} \left\{ \nabla_{\hat{\boldsymbol{u}}_l^q} \Lambda_l^q (\Lambda_l^q)^* \right\} \right], \end{aligned} \tag{26}$$

where $\mathrm{Re}\{\cdot\}$ denotes the real part operation, while the term $\ell(\hat{\boldsymbol{u}}_l^q)$ represents substituting the current estimated value $\hat{\boldsymbol{u}}_l^q$ into (16).

Therefore, the iterative estimation process of the target position by the $l$th local sensor node can be represented as

$$\begin{aligned} \hat{\boldsymbol{u}}_l^{q+1} = \hat{\boldsymbol{u}}_l^q & - \left[ \mathrm{Re} \left\{ \left( \nabla_{\hat{\boldsymbol{u}}_l^q} \Lambda_l^q \right)^* \left( \nabla_{\hat{\boldsymbol{u}}_l^q} \Lambda_l^q \right)^\top \right\} \right]^{-1} \\ & \times \left[ \nabla_{\hat{\boldsymbol{u}}_l^q} \Xi_l^q \ell(\hat{\boldsymbol{u}}_l^q) - \mathrm{Re} \left\{ \nabla_{\hat{\boldsymbol{u}}_l^q} \Lambda_l^q (\Lambda_l^q)^* \right\} \right]. \end{aligned} \tag{27}$$

Each sensor node can iteratively execute the above equation to get the estimate of the target.

At the local sensor nodes, there are multiple potential target positions that maximize the objective function. These potential target positions have equal time delays for the nodes. Moreover, we note that the objective function exhibits convexity only in the vicinity of the true target position. Thus, the iterative convergence to the target true value requires selection of an initial value close to the target true value.

### *B. Initialization Procedure*

We note that to select the initial value of the target position, a rough two-step localization can be adopted. However, due to the poor accuracy of the two-step localization method at low SNRs, there may be significant errors between the selected

initial value of the target position and the true value, thereby affecting the convergence speed of the local iteration process. In this section, a more efficient initialization method based on the PSO algorithm is designed.

Assume that a swarm of $U$ particles explores the initial target position. The $i$th particle $(i = 1,\ldots,U)$ at the $z$th iteration is described by two features: position vector $u_i^z$ and velocity vector $v_i^z$. Define the positive (tunable) constants $h_1$ and $h_2$ as the acceleration coefficients that guide the particles toward the personal best and global best positions, respectively. The velocities and positions of all the particles are updated at each iteration as

$$\begin{aligned} \boldsymbol{v}_i^{z+1} &= H\left[\boldsymbol{v}_i^z + h_1 r_1 \left(\tilde{\boldsymbol{u}}_i^z - \boldsymbol{u}_i^z\right) + h_2 r_2 \left(\bar{\boldsymbol{u}}_i^z - \boldsymbol{u}_i^z\right)\right], \\ \boldsymbol{u}_i^{z+1} &= \boldsymbol{u}_i^z + \boldsymbol{v}_i^{z+1}. \end{aligned} \tag{28}$$

where $\tilde{\boldsymbol{u}}_i^z$ denotes the personal best position achieved by the $i$th particle at the $z$th iteration. The constriction factor $H$ is given by [8]

$$H = \frac{2}{\left|2 - (h_1+h_2) - \sqrt{(h_1+h_2)^2 - 4(h_1+h_2)}\right|}. \tag{29}$$

Note that the terms $r_1$ and $r_2$ are random variables uniformly distributed over $[0,1]$ [8].

The update criterion for the position of the $i$th particle at the $(z+1)$th iteration is

$$\tilde{\boldsymbol{u}}_i^{z+1} = \begin{cases} \tilde{\boldsymbol{u}}_i^z & \zeta\left(\boldsymbol{u}_i^{z+1}\right) \geq \zeta\left(\tilde{\boldsymbol{u}}_i^z\right) \\ \boldsymbol{u}_i^{z+1} & \zeta\left(\boldsymbol{u}_i^{z+1}\right) < \zeta\left(\tilde{\boldsymbol{u}}_i^z\right) \end{cases}, \tag{30}$$

where $\zeta\left(\tilde{\boldsymbol{u}}_i^z\right)$ represents the value of the objective function when $\tilde{\boldsymbol{u}}_i^z$ is substituted into (6). The global best position $\bar{\boldsymbol{u}}^{z+1}$ at the $(z+1)$th iteration is obtained by comparing all the personal best positions updated by particles until the $k$th iteration, namely,

$$\begin{aligned} \bar{\boldsymbol{u}}^{z+1} &= \tilde{\boldsymbol{u}}_{i^*}, \\ i^* &= \underset{i\in\{1,\ldots,U\}}{\arg\max}\ \zeta\left(\tilde{\boldsymbol{u}}_i^z\right). \end{aligned} \tag{31}$$

For computational efficiency, we constrain the potential search region of the target location to the surveillance area of the sensors, defined as $[\boldsymbol{u}_{min}, \boldsymbol{u}_{max}]$, where $\boldsymbol{u}_{min} = [x_{min}, y_{min}]^\top$ and $\boldsymbol{u}_{max} = [x_{max}, y_{max}]^\top$ are determined by the range of the surveillance area. Note that it is possible for some particles to move outside $[\boldsymbol{u}_{min}, \boldsymbol{u}_{max}]$ during the iteration process. To avoid this, we impose the following step in iterations to constrain its range:

$$\boldsymbol{u}_i^{z+1} = \begin{cases} \boldsymbol{u}_{max} & \boldsymbol{u}_i^{z+1} > \boldsymbol{u}_{max} \\ \boldsymbol{u}_{min} & \boldsymbol{u}_i^{z+1} < \boldsymbol{u}_{min} \end{cases}. \tag{32}$$

The above steps are repeated until $z$ reaches the maximum number of iterations $Z$.

### C. Fusion Strategy

The aforementioned local iterative estimation process, while capable of obtaining the estimate of the target position locally, is limited by the performance of individual sensors, making it challenging to achieve satisfactory localization results. In this subsection, consensus is employed to enhance the estimation performance of individual nodes. The consensus method is an effective decentralized fusion strategy where each node aggregates relevant information from its one-hop neighbors about unknown parameters in the system to improve the local performance.

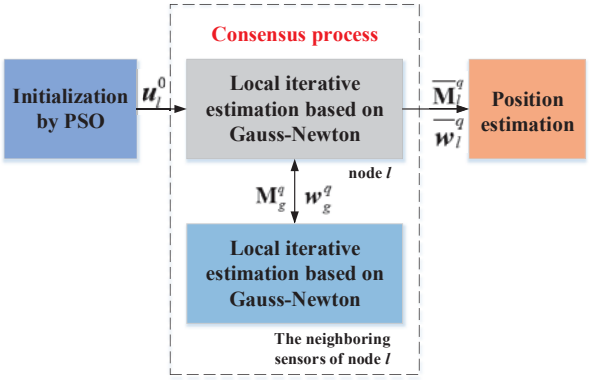


Fig. 2. The flowchart of DDL at the $l$th node.

Here, we propose to employ the average consensus approach [18], [19]. It relies on iteratively refining the local estimates at nodes and exchanging information with one-hop neighbors to collaboratively estimate a shared target position. After computing the local gradient at each sensor, consensus is reached by exchanging information with neighbors. The update rule for each consensus step is as

$$\bar{\mathbf{M}}_l^q = \frac{1}{G}\sum_{g\in\aleph_l} \mathbf{M}_g^q, \quad \bar{\boldsymbol{w}}_l^q = \frac{1}{G}\sum_{g\in\aleph_l} w_g^q, \tag{33}$$

where $\aleph_l$ represents the set of neighbors of sensor $l$ excluding itself, $G$ is the number of elements in $\aleph_l$, while

$$\begin{aligned} \mathbf{M}_g^q &= \mathrm{Re}\left\{\left(\nabla_{\hat{\boldsymbol{u}}_g^q}\Lambda_g^q\right)^*\left(\nabla_{\hat{\boldsymbol{u}}_g^q}\Lambda_g^q\right)^\top\right\}, \\ \boldsymbol{w}_g^q &= \nabla_{\hat{\boldsymbol{u}}_g^q}\Xi_g^q\ell(\hat{\boldsymbol{u}}_g^q) - \mathrm{Re}\left\{\nabla_{\hat{\boldsymbol{u}}_g^q}\Lambda_g^q(\Lambda_g^q)^*\right\}. \end{aligned} \tag{34}$$

After reaching consensus, each local sensor can execute Gauss-Newton iterations as follows to obtain an estimate of the target position,

$$\hat{\boldsymbol{u}}_l^{q+1} = \hat{\boldsymbol{u}}_l^q - \left(\bar{\mathbf{M}}_l^q\right)^{-1}\bar{\boldsymbol{w}}_l^q. \tag{35}$$

Up to this point, we have derived the entire DDL method using average consensus. At its core, each sensor node generates intermediate information $\bar{\mathbf{M}}_l^q$ and $\bar{\boldsymbol{w}}_l^q$ through a localized iterative estimation process. These intermediate pieces of information are then shared with the neighboring nodes using an averaging consensus strategy. Once a consensus is reached, the target position estimation is complete utilizing the local iterative process. The flowchart of the proposed DDL algorithm is shown in Fig. 2.

TABLE I
SYSTEMATIC COORDINATE PARAMETERS

| Label | Location (m) | Label | Location (m) |
|---|---|---|---|
| Node 1 | $(2,5)$ | Node 5 | $(10,18)$ |
| Node 2 | $(18,18)$ | Node 6 | $(17,2)$ |
| Node 3 | $(3,10)$ | Node 7 | $(10,12)$ |
| Node 4 | $(15,10)$ | Node 8 | $(12,6)$ |

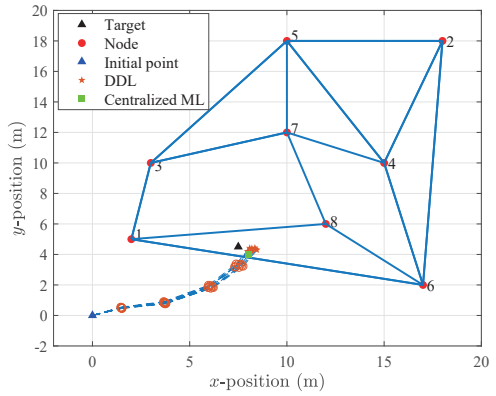


Fig. 3. Conceptual diagram of the consensus process in a decentralized multi-sensor system, where the red circles represent the target position estimates generated by different sensors in various consensus rounds. The blue lines connecting the sensors represent the communication link between the two nodes. Note that each node can only communicate with its one-hop neighbors.

## V. PERFORMANCE ASSESSMENT

In this section, some numerical simulations are performed to examine the performance of the proposed DDL method. Consider a decentralized localization network composed of 8 sensor nodes as shown in Fig. 3. The coordinates of the sensor nodes are listed in Table I, and the unknown radiation source is located at $(7.5, 4.5)$ m. As mentioned earlier, the entire system is assumed to be synchronized. The sensor emits a linear frequency modulated continuous wave signal with a transmission bandwidth of 40 MHz and a sampling rate of 320 MHz. The false alarm rate is set as $P_{fa} = 10^{-2}$. During the execution process of the PSO algorithm in the initialization determination process, the acceleration coefficients $h_1$ and $h_2$ are both selected as 2.05 [8]. Inserting them into (29) yields $H = 0.7298$. The root mean square error (RMSE) is used as the performance metric for individual sensor localization. The RMSE of the estimator $\hat{\boldsymbol{\theta}} = [\hat{x}, \hat{y}]^\top$ is defined as

$$\text{RMSE}(\hat{\boldsymbol{\theta}}) = \sqrt{\frac{1}{E}\sum_{i=1}^{E}\left[(x_i - \hat{x}_i)^2 + (y_i - \hat{y}_i)^2\right]}, \tag{36}$$

where $[x_i, y_i]^\top$ represents the true position of the target in the $i$th experiment, $[\hat{x}_i, \hat{y}_i]^\top$ is the estimated position of the target, and $E$ denotes the number of experiments. The results are obtained by averaging over $1,000$ Monte Carlo realizations. The average localization error is adopted as the performance metric for the decentralized system. As a comparison, we designate the traditional grid-search-based centralized direct localization method as "centralized ML".

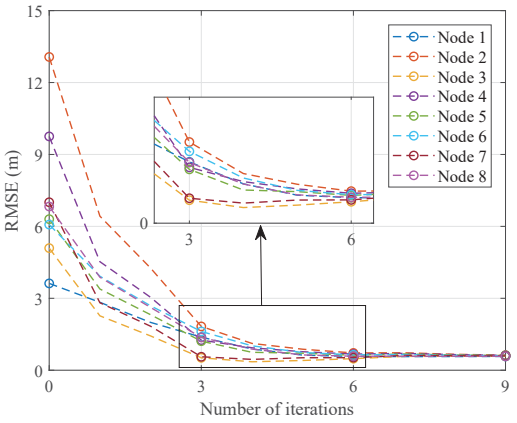


Fig. 4. Variations in the localization performance against the number of iterations at different sensor nodes.

Figure 3 illustrates the consensus process of the proposed DDL algorithm. In the figure, we can observe the evolution of the position estimates of each sensor node as the algorithm iterates. It is noteworthy that all sensors follow trajectories approaching the centralized solution. As the number of consensus rounds increases, the estimates of sensors converge increasingly towards the same (centralized ML) solution.

Figure 4 shows the variation in the localization performance of individual sensor nodes over iteration cycles. It can be observed that the localization performance of nodes in decentralized networks is not only related to the distance between nodes and targets but also to the number of neighbors and the distance between neighbors and the target. Specifically, when the number of iterations is small, the more neighbors a node has and the closer it is to the target, the better its localization performance is. With the gradual increase of the number of iterations, the influence of the number of neighbors is reduced, and basically the smaller the distance, the better the performance. When the number of iterations is sufficient, the localization performance of each sensor gradually improves and converges to a steady state. Furthermore, the localization performance of each sensor is very similar, demonstrating a steady-state performance.

In Fig. 5, in order to compare the localization performance of the proposed DDL method and the centralized ML method, we introduce the measure of average localization error, which is defined as follows

$$\text{Average Localization Error} = \frac{1}{L}\sum_{l=1}^{L}\text{RMSE}_l(\hat{\boldsymbol{\theta}}), \tag{37}$$

where $\text{RMSE}_l(\hat{\boldsymbol{\theta}})$ represents the localization error of the $l$th node, as defined by (36). It can be observed that, although there is some performance difference between the DDL method and the centralized ML method in the initial consensus stages, as the number of consensus rounds increases, the localization performance of the proposed DDL method gradually converges to that of the centralized ML method. This indicates that, in the absence of FC participation, the proposed DDL method

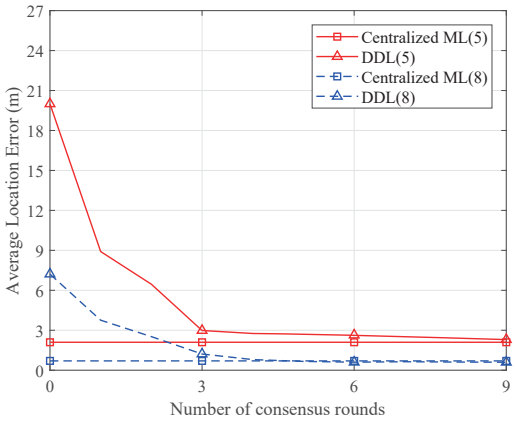


Fig. 5. Average localization error of the proposed DDL method and the centralized ML method, where the numbers inside the parentheses represent the number of sensors.

can achieve performance comparable to the centralized direct localization method. Additionally, it can be observed that as the number of sensors participating in consensus increases, the localization performance of the decentralized system also improves accordingly.

## VI. Conclusion

To address the issues of high communication load and poor robustness in centralized direct localization methods, we developed a decentralized direct localization method. Each sensor first employs the Gauss-Newton method locally to obtain iterative estimates of the target position. Through information exchange with neighboring sensors and by employing a consensus approach, comparable performance to centralized direct localization methods was achieved. Our simulation results validated the effectiveness of the proposed method, indicating that it not only enhances the robustness of the system but it also reduces the communication load.

## Acknowledgments

This work was supported in part by the National Natural Science Foundation of China under Grant 62231008 and 62301127, in part by the China Postdoctoral Science Foundation under Grant BX20220057, 2023M730509 and GZB20230112, the "Tianfu Qingcheng" Plan of Sichuan Province under Grant1332 and 1395.

The work of H. Q. Ngo was supported by the U.K. Research and Innovation Future Leaders Fellowships under Grant MR/X010635/1, and a research grant from the Department for the Economy Northern Ireland under the US-Ireland R&D Partnership Programme.

The work of M. Matthaiou was supported by the European Research Council (ERC) under the European Union's Horizon 2020 research and innovation programme (grant agreement No. 101001331).

## References

[1] B. Khaleghi, A. Khamis, F. O. Karray, and S. N. Razavi, "Multisensor data fusion: A review of the state-of-the-art," *Inf. Fusion.*, vol. 14, no. 1, pp. 28-44, 2013.

[2] D. Ciuonzo, P. S. Rossi and P. Willett, "Generalized Rao test for decentralized detection of an uncooperative target," *IEEE Signal Process. Lett.*, vol. 24, no. 5, pp. 678-682, May 2017.

[3] Y. Zheng, N. Cao, T. Wimalajeewa and P. K. Varshney, "Compressive sensing based probabilistic sensor management for target tracking in wireless sensor networks," *IEEE Trans. Signal Process.*, vol. 63, no. 22, pp. 6049-6060, Nov. 2015.

[4] A. RamÃ■rez-Arroyo, A. Alex-Amor, P. Padilla and J. F. Valenzuela-ValdÃl's, "Joint direction-of-arrival and time-of-arrival estimation with ultra-wideband elliptical arrays," *IEEE Trans. Wireless Commun.*, vol. 22, no. 12, pp. 9187-9200, Dec. 2023.

[5] S. Zhu and Z. Ding, "Distributed cooperative localization of wireless sensor networks with convex hull constraint," *IEEE Trans. Wireless Commun.*, vol. 10, no. 7, pp. 2150-2161, Jul. 2011.

[6] A. A. Ababneh, "Density-based sensor selection for RSS target localization," *IEEE Sensors J.*, vol. 18, no. 20, pp. 8532-8540, Oct. 2018.

[7] B. C. Tedeschini, M. Brambilla, L. Barbieri and M. Nicoli, "Addressing data association by message passing over graph neural networks," in *Proc. ISIF FUSION*, Jul. 2022, pp. 01-07.

[8] G. Zhang, W. Yi, P. K. Varshney and L. Kong, "Direct target localization with quantized measurements in noncoherent distributed MIMO radar systems," *IEEE Trans. Geosc. Remote Sens.*, vol. 61, no. C, pp. 1-18, Apr. 2023.

[9] A. Weiss, "Direct position determination of narrowband radio frequency transmitters," *IEEE Signal Process. Lett.*, vol. 11, no. 5, pp. 513-516, Apr. 2004.

[10] H. Godrich, A. M. Haimovich, and R. S. Blum, "Target localization accuracy gain in MIMO radar-based systems," *IEEE Trans. Inf. Theory.*, vol. 56, no. 6, pp. 2783-2803, May 2010.

[11] J. Lee and C. Tepedelenlioglu, "Distributed detection in coexisting large-scale sensor networks," *IEEE Sensors J.*, vol. 14, no. 4, pp. 1028-1034, Apr. 2014.

[12] F. S. Cattivelli and A. H. Sayed, "Diffusion LMS strategies for distributed estimation," *IEEE Trans. Signal Process.*, vol. 58, no. 3, pp. 1035-1048, Mar. 2010.

[13] S. Tomic, M. Beko and R. Dinis, "Distributed RSS-AoA based localization with unknown transmit powers," *IEEE Wireless Commun. Lett.*, vol. 5, no. 4, pp. 392-395, Aug. 2016.

[14] M. Xie, W. Yi, T. Kirubarajan and L. Kong, "Joint node selection and power allocation strategy for multitarget tracking in decentralized radar networks," *IEEE Trans. Signal Process.*, vol. 66, no. 3, pp. 729-743, Feb. 2018.

[15] T. Zhao and A. Nehorai, "Information-driven distributed maximum likelihood estimation based on Gauss-Newton method in wireless sensor networks," *IEEE Trans. Signal Process.*, vol. 55, no. 9, pp. 4669-4682, Sept. 2007.

[16] V. Matta, P. Braca, S. Marano and A. H. Sayed, "Diffusion-based adaptive distributed detection: steady-state performance in the slow adaptation regime," *IEEE Trans. Inf. Theory.*, vol. 62, no. 8, pp. 4710-4732, Aug. 2016.

[17] R. Forsling, Z. Sjanic, F. Gustafsson and G. Hendeby, "Consistent distributed track fusion under communication constraints," in *Proc. ISIF FUSION*, Jul. 2019, pp. 1-8.

[18] G. Soatti, M. Nicoli, S. Savazzi and U. Spagnolini, "Consensus-based algorithms for distributed network-state estimation and localization," *IEEE Trans. Signal Inf. Process. Netw.*, vol. 3, no. 2, pp. 430-444, Jun. 2017.

[19] M. Wu, N. Xiong and L. Tan, "Adaptive range-based target localization using diffusion Gauss-Newton method in industrial environments," *IEEE Trans. Ind. Inform.*, vol. 15, no. 11, pp. 5919-5930, Nov. 2019.

[20] W. Xia and W. Liu, "Distributed adaptive direct position determination of emitters in sensor networks," *Signal Process.*, vol. 123, no. C, pp. 100-111, 2016.

[21] M. Pourhomayoun and M. L. Fowler, "Distributed computation for direct position determination emitter location," *IEEE Trans. Aerosp. Electron. Syst.*, vol. 50, no. 4, pp. 2878-2889, Oct. 2014.

[22] F. Ma, Z.-M. Liu and F. Guo, "Distributed direct position determination," *IEEE Trans. Veh. Technol.*, vol. 69, no. 11, pp. 14007-14012, Nov. 2020.